

# Bistability and switching in the lysis/lysogeny genetic regulatory network of bacteriophage $\lambda$

Tianhai Tian, Kevin Burrage\*

Department of Mathematics, Advanced Computational Modelling Centre, University of Queensland, Brisbane, Qld 4072, Australia

Received 27 April 2003; received in revised form 11 August 2003; accepted 4 November 2003

## Abstract

Bistability and switching are two important aspects of the genetic regulatory network of  $\lambda$  phage. Positive and negative feedbacks are key regulatory mechanisms in this network. By the introduction of threshold values, the developmental pathway of  $\lambda$  phage is divided into different stages. If the protein level reaches a threshold value, positive or negative feedback will be effective and regulate the process of development. Using this regulatory mechanism, we present a quantitative model to realize bistability and switching of  $\lambda$  phage based on experimental data. This model gives descriptions of decisive mechanisms for different pathways in induction. A stochastic model is also introduced for describing statistical properties of switching in induction. A stochastic degradation rate is used to represent intrinsic noise in induction for switching the system from the lysogenic pathway to the lysis pathway. The approach in this paper represents an attempt to describe the regulatory mechanism in genetic regulatory network under the influence of intrinsic noise in the framework of continuous models.

© 2003 Elsevier Ltd. All rights reserved.

**Keywords:** Genetic regulatory networks; Stochastic simulation; Bistability; Switching;  $\lambda$  bacteriophage

## 1. Introduction

$\lambda$  phage is a virus that infects the bacterium *Escherichia coli*. It is called a temperate phage because it can be in the form of either lysis or lysogen. In the lysogenic form, the virus will replicate passively whenever the host bacterium replicates. Under the right conditions, a lysogen can be induced from the lysogenic pathway to the lysis pathway.  $\lambda$  phage has been studied extensively because it is one of the simplest developmental switches (Ptashne et al., 1980; Maurer et al., 1980; Meyer et al., 1980; Johnson et al., 1981; Ptashne, 1992). It is also an organism that exhibits probabilistic or stochastic behaviour. In the emerging field of genetic network analysis, the  $\lambda$  regulatory network has often been used as a testing ground for modelling methodology (Dodd et al., 2001; Hasty et al., 2001b).

Mathematical models for the genetic regulatory network of  $\lambda$  phage can be classified into deterministic or stochastic models. Based on detailed biochemical reactions, kinetic models with ordinary differential

equations have been used for describing protein concentrations (Ackers et al., 1982; Shea and Ackers, 1985; Reinitz and Vaisnys, 1990). In addition, stochastic kinetic models have been studied for describing intrinsic noise due to low molecular numbers in a cell by means of the stochastic simulation algorithm (Arkin et al., 1998; McAdams and Arkin, 1997), and for describing external noise due to environmental fluctuations by using stochastic differential equations (Hasty et al., 2000, 2001a).

Theoretically, abstract models can be constructed in order to get insight into the behaviour of entire classes of biological systems (Smolen et al., 2000). The validity of mathematical models should be assessed by comparing the theoretical prediction with experimentally determined values. The use of experimental data is regarded as one of the key factors in the success of mathematical modelling. Unfortunately, extant kinetic models of  $\lambda$  phage exhibit no bistability property with experimentally estimated values. Although the existence of bistability has been realized by a simplified model (Hasty et al., 2001a) recently, bistability properties disappear if a more detailed model and experimentally estimated data are employed. The possible reason may be due to some importantly omitted aspects of the

\*Corresponding author. Tel.: +61-7-33653487; fax: +61-7-33656136.

E-mail address: [kb@maths.uq.edu.au](mailto:kb@maths.uq.edu.au) (K. Burrage).

switching regulatory mechanism in the standard ‘word model’ or in the mathematical model (Hasty et al., 2001b; Reinitz and Vaisnys, 1990). For example, strong positive feedback, which is always effective in extant models, will lead all simulations to the lysogenic pathway. Thus conditions for the effectiveness of feedback mechanisms in biological systems should be realized in mathematical models. This is one of the motivations of this paper.

Noise exists in biological systems due to environmental fluctuations and the inherent stochastic nature of biochemical processes. It has been proposed that noise in the form of random fluctuations arises in biological networks in one of two ways: namely as internal noise or external noise (Hasty et al., 2000, 2001a). However, living systems are optimized to function in the presence of stochastic fluctuations (Thattai and van Oudenaarden, 2001), and biochemical networks must withstand considerable variations and random perturbations of biochemical parameters (Becskei and Serrano, 2000). Such a property of biological systems is known as robustness (Barkai and Leibler, 1997; Alon et al., 1999; Gardner and Collins, 2000; Gonze et al., 2002). On the other hand, biological systems are also sensitive to environmental fluctuations and/or intrinsic noise in certain time periods. For example, noise in gene expression could lead to qualitative differences in a cell’s phenotype if the expressed genes act as inputs to downstream regulatory thresholds (McAdams and Arkin, 1997). Another example arises when an infecting  $\lambda$  phage determines a pathway to follow (Ptashne et al., 1980; Ptashne, 1992). Mathematical models should be able to not only withstand random perturbations in model parameters for stable biological systems but also have the ability to describe different pathways in order to explain phenotypic properties.

In this paper a new modelling methodology is introduced by considering threshold values. We present a quantitative model for  $\lambda$  phage that allows bistability and switching of the genetic regulatory network based on experimental data. Finally a stochastic model is also presented based on the representation of intrinsic noise for studying the switching from the lysogenic to the lysis pathway.

## 2. Mathematical models

Mathematical models discussed here are used to describe the principle of the  $\lambda$  right operator control system and the actions of regulatory proteins CI repressor and cro. The operator region  $O_R$  consists of 3 binding sites designated  $O_{R1}$ ,  $O_{R2}$  and  $O_{R3}$ , and is situated between the promoters  $P_{RM}$  and  $P_R$  for genes  $cI$  and  $cro$ , respectively. The dimeric forms of repressor and cro bind to these binding sites to regulate the

transcription of genes  $cI$  and  $cro$  (Ptashne et al., 1980; Meyer et al., 1980; Ptashne, 1992).

The deterministic model presented in this section is based on the lysogenic and lysis states of the  $\lambda$  phage system. The lysogenic state is mainly regulated by the  $P_{RM}$  promoter and  $cI$  gene. Cooperative binding of CI dimers at  $O_{R1}$  and  $O_{R2}$  represses the  $P_R$  promoter, which blocks the transcription of gene  $cro$ . Binding of CI dimer to  $O_{R2}$  stimulates the intrinsically weak promoter for the  $cI$  gene, which is known as the positive feedback of the  $cI$  gene. Binding of the CI dimer to  $O_{R3}$ , when at high repressor concentration, will repress the transcription of its own gene. This regulatory mechanism is called negative feedback.

On the other hand, the lysis state is mainly determined by the  $P_R$  promoter and  $cro$  gene. When cro dimer binds to the operator site  $O_{R3}$ , the activity in  $P_{RM}$  is repressed and the transcription from  $P_R$  is turned on. Following a burst of synthesis of cro protein, cro at high concentration will turn off transcription from  $P_R$  by the cro dimers binding to  $O_{R1}$  and/or  $O_{R2}$  operator sites. This is known as the negative feedback of the  $cro$  gene.

Biochemical reactions in this system are classified into fast reactions which are assumed to be in an equilibrium state and slow reactions which represent transcription and degradation. Fast reactions include two monomer–dimer reactions and binding reactions of ligands to the promoter sites. A complete list of the possible configurations of  $O_R$  was presented by Shea and Ackers (1985). Let  $R_2$ ,  $C_2$  and RNAP denote the repressor dimer, cro dimer and RNA polymerase, respectively. These three ligands can bind to the  $O_R$  promoter region. Here Table 1 gives these 40 configurations using the table format in Reinitz and Vaisnys (1990) but the values of the free energy  $\Delta G_s$  come from the updated values in Darling et al. (2000).

Let  $R$  and  $C$  denote the repressor and cro proteins. The interactions between monomers and dimers are of the form (Hasty et al., 2000, 2001a; Arkin et al., 1998)



and we have

$$[R_2] = K_r x^2, \quad [C_2] = K_c y^2,$$

where  $x = [R]$  and  $y = [C]$  are concentrations of repressor and cro, respectively. The dimerization constants are  $K_r = 0.05 \text{ nM}^{-1}$  (Ptashne, 1992; Hasty et al., 2001a) and  $K_c = 0.0307 \text{ nM}^{-1}$  (Darling et al. 2000).

The increments of protein concentrations  $x$  and  $y$  are the difference between the synthesis from transcription and degradation. Based on the complete list of 40 configurations, Reinitz and Vaisnys (1990) introduced a

Table 1  
Binding states of  $O_R$  and free energy for each configuration

State	$P_{RM}$	$O_{R3}$	$O_{R2}$	$O_{R1}$	$P_R$	$\Delta G_s$	$i(s)$	$j(s)$	$k(s)$
1						0.0	0	0	0
2				$R_2$		−12.5	1	0	0
3			$R_2$			−10.5	1	0	0
4		$R_2$				−9.5	1	0	0
5			$R_2$	$R_2$		−25.7	2	0	0
6		$R_2$		$R_2$		−22	2	0	0
7		$R_2$	$R_2$			−22.9	2	0	0
8		$R_2$	$R_2$	$R_2$		−35.2	3	0	0
9				$C_2$		−12.0	0	1	0
10			$C_2$			−10.8	0	1	0
11		$C_2$				−13.4	0	1	0
12			$C_2$	$C_2$		−23.8	0	2	0
13		$C_2$		$C_2$		−25.4	0	2	0
14		$C_2$	$C_2$			−24.8	0	2	0
15		$C_2$	$C_2$	$C_2$		−37.1	0	3	0
16			$C_2$	$R_2$		−23.3	1	1	0
17		$C_2$		$R_2$		−25.9	1	1	0
18		$C_2$	$C_2$	$R_2$		−37.3	1	2	0
19		$C_2$	$R_2$			−23.9	1	1	0
20			$R_2$	$C_2$		−22.5	1	1	0
21		$C_2$	$R_2$	$C_2$		−35.9	1	2	0
22		$R_2$	$C_2$			−20.3	1	1	0
23		$R_2$		$C_2$		−21.5	1	1	0
24		$R_2$	$C_2$	$C_2$		−33.3	1	2	0
25		$C_2$	$R_2$	$R_2$		−39.1	2	1	0
26		$R_2$	$C_2$	$R_2$		−32.8	2	1	0
27		$R_2$	$R_2$	$C_2$		−34.9	2	1	0
28					$RNAP$	−12.5	0	0	1
29		$R_2$			$RNAP$	−22.0	1	0	1
30		$C_2$			$RNAP$	−25.9	0	1	1
31	$RNAP$		$R_2$			−22.0	1	0	1
32	$RNAP$		$R_2$	$R_2$		−37.2	2	0	1
33	$RNAP$		$R_2$	$C_2$		−34.0	1	1	1
34	$RNAP$					−11.5	0	0	1
35	$RNAP$			$R_2$		−24.0	1	0	1
36	$RNAP$			$C_2$		−23.5	0	1	1
37	$RNAP$	$C_2$				−22.3	0	1	1
38	$RNAP$	$C_2$	$R_2$			−34.8	1	1	1
39	$RNAP$	$C_2$	$C_2$			−35.3	0	2	1
40	$RNAP$				$RNAP$	−24.0	0	0	2

model for this system, given by

$$\begin{aligned}\frac{dx}{dt} &= S_x P_x(x, y) - k_{dx} x, \\ \frac{dy}{dt} &= S_y P_y(x, y) - k_{dy} y\end{aligned}\quad (2)$$

with

$$\begin{aligned}P_x(x, y) &= \alpha(f_{31} + f_{32} + f_{33}) + \sum_{m=34}^{40} f_m, \\ P_y(x, y) &= f_{28} + f_{29} + f_{30} + f_{40}\end{aligned}$$

and

$$\begin{aligned}f_s &= \frac{K_s(K_r x^2)^{i(s)}(K_c y^2)^{j(s)}[RNAP]^{k(s)}}{\sum_{m=1}^{40} K_m(K_r x^2)^{i(m)}(K_c y^2)^{j(m)}[RNAP]^{k(m)}}, \\ K_s &= \exp(\Delta G_s / RT).\end{aligned}$$

Here  $S_x$  and  $S_y$  are the synthesis rates of repressor and cro, respectively,  $k_{dx}$  and  $k_{dy}$  are the degradation rates for repressor and cro, respectively,  $f_s$  is defined by the  $s$ -th configuration in Table 1,  $K_s$  is the equilibrium constant with the free energy  $\Delta G_s$  listed in Table 1 and  $\alpha = 11$  is the indication of positive feedback of the repressor. In addition, the universal gas constant is  $R = 1.99 \text{ cal mol deg}^{-1}$  and the absolute temperature is  $T = 310 \text{ K}$ . The synthesis rates and degradation rates are from Reinitz and Vaisnys (1990), namely  $S_x = 6.0 \text{ nM min}^{-1}$ ,  $S_y = 4.7 \text{ nM min}^{-1}$ ,  $k_{dx} = 1.732 \times 10^{-2} \text{ min}^{-1}$ ,  $k_{dy} = 4.042 \times 10^{-2} \text{ min}^{-1}$  and the concentration of RNAP remains constant, namely  $[RNAP] = 30 \text{ nM}$ . Note that the monomer–dimer reactions (1) are different from those in Reinitz and Vaisnys (1990) due to some updated values. The major difference between model (2) and that in Hasty et al., (2001a) is that the complete list of configurations is used.

### 3. Threshold values

Using model (2) together with the parameter values given in Section 2, numerical simulations indicate that bistability does not exist in this system with the given values. The lysis steady state does not exist and all the simulations lead to the lysogenic state for any given initial condition. We also simulated this system with the same control variables and varied the synthesis rates  $k_{tx}$  and  $k_{ty}$ . Bistability exists only when  $k_{ty} \geq 51$  for a fixed synthesis rate  $k_{tx} = 6.0$ , or when  $k_{tx} \leq 1.4$  for a fixed synthesis rate  $k_{ty} = 4.7$ . This suggests that certain aspects of regulation in this system have been neglected.

The main difficulty of this differential equation model is the assumption of continuity for protein concentrations, which is valid if the numbers of molecules are large. For biochemical reactions with small numbers of reactants, the stochastic simulation algorithm (SSA) (Gillespie, 1977) is an efficient approach for simulating biochemical reactions within cells. In this approach, biochemical processes are treated as discrete and the occurrence of a specific reaction is determined by a stochastic process. Recently the  $\tau$ -leap method has been proposed for improving the efficiency of SSA (Gillespie, 2001). For a chemical reaction system with  $N$  molecular species and  $M$  reaction channels, we can define a propensity function  $a_j(X)$  for the  $j$ -th reaction channel which is a function of the current state  $X$  at time  $t$ . The number of times that the  $j$ -th reaction channel occurs in the time interval  $[t, t + \tau)$  is given by

$$K_j(\tau; X, t) = P(a_j(X)\tau), \quad (3)$$

where  $P(a_j(X)\tau)$  is a Poisson random variable with mean  $a_j(X)\tau$ . The  $\tau$ -leap method gives increments of the system in each time subinterval, which is similar to the explicit Euler method for solving ordinary differential

equations. Now we use this principle to simulate biological reactions with low protein concentrations in the framework of continuous models.

According to thermodynamics theory, binding equilibrium coefficients are constants that have been used in extant modelling (Shea and Ackers, 1985; Reinitz and Vaisnys, 1990; Hasty et al., 2000, 2001a). However, it would be not appropriate to apply this thermodynamics theory directly to the system of  $\lambda$  phage where the concentrations of CI and cro are low. Inspired by the assumption of using functions for synthesis and degradation rates rather than constants (Reinitz and Vaisnys, 1990), we use functions to indicate binding strengths and synthesis rates at different developmental stages due to the different possibilities of the biochemical reactions. Here we will concentrate on two important regulatory mechanisms: positive and negative feedbacks. Similar approaches can also be applied to other mechanisms.

The lysogenic pathway can be divided into three developmental stages: the weak promoter stage with low CI concentration, the fast growth stage stimulated by positive feedback with dimers binding to  $O_R1$  and  $O_R2$ , and the repressed growth stage regulated by negative feedback with dimers binding to the three operator sites. There are two components of the weak promoter stage, namely in establishing the lysogenic pathway and in induction. The first case occurs when the CII protein causes polymerase to transcribe the *cI* gene from the promoter  $P_{RM}$ . Here we just discuss the second case which is associated with the synthesis rate  $S_x$  for the repressor.

In induction, the rate of repressor synthesis drops as repressor dimers vacate  $O_R1$  and  $O_R2$  when the repressor concentration has dropped about fivefold (Ptashne, 1992). As the repressor dimers bind to operator sites  $O_R1$  and  $O_R2$  virtually simultaneously, due to the cooperativity of repressor binding, positive feedback will be effective if the CI concentration is high enough for tight binding of the CI dimer to the operator site  $O_R1$ . Thus it would be better to use a functional synthesis rate to indicate these two different stages.

We assume that the synthesis rate  $\bar{S}_x$  reaches constant value  $S_x$  (the maximum) if the repressor concentration exceeds a certain value  $x_1^*$ . However, when repressor concentration is below  $x_1^*$ , it is supposed that the synthesis rate is a function of the repressor concentration. For simplicity, the synthesis rate is assumed to be a linear function with value 0 at  $x = 0$  and value  $S_x$  at  $x = x_1^*$ . This consideration leads to the following synthesis rate, given by

$$\bar{S}_x = \begin{cases} S_x, & x \geq x_1^*, \\ S_x x / x_1^*, & x < x_1^*. \end{cases} \quad (4)$$

On the other hand, a constant cro synthesis rate  $S_y$  is used here. The reason for this assumption is due to the single burst synthesis of cro protein if the lysis pathway is established.

The next function is associated with binding reaction to the operator site  $O_R3$ . Over a broad range of concentrations including that found in lysogen,  $O_R1$  and  $O_R2$  are filled and  $O_R3$  is usually vacant. Only at high repressor concentrations do the repressor dimers bind to  $O_R3$  and turn off  $P_{RM}$  (Ptashne et al., 1980). In addition,  $O_R3$  is filled gradually as the repressor concentration is increased (Maurer et al., 1980). Thus the process of the binding reaction for repressor dimer to  $O_R3$  is divided into two stages according to the repressor concentration. When the CI concentration is under a certain value, denoted by  $x < x_2^*$ , the value of the propensity function for the binding reaction to  $O_R3$  is relatively small compared with the values of propensity functions of other reactions and the generated Poisson numbers for the times of binding reaction of CI dimer to  $O_R3$  are likely to be zero. This means this reaction is unlikely to occur with such a CI concentration. In this case we mathematically treat these relatively small probabilities to be 0 as the reaction seldom occur in the biological system at that state condition.

When CI concentration is above the value  $x_2^*$ , the binding strength of CI dimer to  $O_R3$  will increase gradually in accordance with the increase of the repressor concentration. With the assumed threshold value  $x_2^*$ , the binding strength for configuration 8 is of the form

$$\bar{K}_8 = \frac{K_8}{k_x} (x - x_2^*)^+ = \begin{cases} \frac{K_8}{k_x} (x - x_2^*), & x > x_2^*, \\ 0, & x \leq x_2^*, \end{cases}$$

where  $K_8$  is the equilibrium constant defined by the free energy  $\Delta G_8$  in Table 1, and  $k_x$  is a parameter to indicate the possible concentration range in which the negative feedback will be effective. Note that, for all possible concentrations  $x$  predicted by model (2), we choose  $k_x$  in order that  $x \leq x_2^* + k_x$  and so  $\bar{K}_8 \leq K_8$ .

As configurations 4, 6 and 7 are also associated with the negative feedback of repressor, this regulatory mechanism should also be applied to these configurations, namely for  $s = 4, 6, 7$

$$\bar{K}_s = \frac{K_s}{k_x} (x - x_2^*)^+. \quad (5)$$

Now we discuss the threshold values  $x_1^*$  and  $x_2^*$ . The relative concentrations of repressor dimers required to fill the corresponding binding sites on half of the wild-type DNA molecules are 25 for  $O_R3$ , 2 for  $O_R2$  and 1 for  $O_R1$  (Ptashne et al., 1980). Here a value of 1 is assigned for  $O_R1$  as the standard. In addition, in a lysogen state which contains 200–250 monomers of repressor, repressor dimers are typically bound at  $O_R1$  and  $O_R2$  but not



$O_R3$  (Ptashne et al., 1980; Reinitz and Vaisnys, 1990). Thus we choose  $x_1^* = 250$  nM and  $k_x = 120$  because the concentration of the repressor, predicted by model (2), is 370 nM in the lysogenic steady state. In addition  $x_2^* = 50$  which is 20% of  $x_1^*$ . These two threshold values are consistent with the values 1 for  $O_R1$  and 25 for  $O_R3$ .

Similar regulatory mechanism can be applied to the negative feedback of cro protein which is associated with binding reactions of cro dimers to operator sites  $O_R1$  and/or  $O_R2$ . Since cro at high concentration will turn off transcription from  $P_R$ , binding reactions to operator sites  $O_R1$  and  $O_R2$  occur after cro concentration reaches an assumed threshold value  $y^*$ . It is assumed that for  $s = 9, 10, 12, 13, 14, 15$

$$\bar{K}_s = \frac{K_s}{k_y} (y - y^*)^+, \quad (6)$$

where the  $K_s$  are equilibrium constants defined by the free energy in Table 1, and  $k_y$  is a parameter to indicate the possible concentration range in which the negative feedback will be effective. As it is hard to find any quantitative study of cro protein level after lysogenic induction, we use the predicted level derived by a mathematical model (Shea and Ackers, 1985). The cro production rate reaches the maximum when the cro level is 70 nM and the cro concentration is 140 when it is 1 h after the induction. So it is supposed that  $y^* = 70$  nM and  $k_y = 70$ .

The effect of the threshold values in negative feedback mechanisms is that rather than the concentrations going more slowly to their steady states there is a burst of concentration and a more rapid movement to these steady states. It should be noticed that the assumptions underlying the reaction rates in Eqs. (5) and (6) realize biochemical reactions with small probabilities. Certainly, this consideration can be applied to other binding reactions listed in Table 1. Here we concentrate only on the positive and negative feedbacks that are the most important regulatory mechanisms for bistability and genetic switching.

Based on the discussion above, the model with threshold values is

$$\begin{aligned} \frac{dx}{dt} &= \bar{S}_x \bar{P}_x(x, y) - k_{dx} x, \\ \frac{dy}{dt} &= S_y \bar{P}_y(x, y) - k_{dy} y, \end{aligned} \quad (7)$$

where  $\bar{S}_x$  is defined by Eq. (4) and the functions  $\bar{P}_x(x, y)$  and  $\bar{P}_y(x, y)$  are given by

$$\begin{aligned} \bar{P}_x(x, y) &= \alpha (\bar{f}_{31} + \bar{f}_{32} + \bar{f}_{33}) + \sum_{m=34}^{40} \bar{f}_m, \\ \bar{P}_y(x, y) &= \bar{f}_{28} + \bar{f}_{29} + \bar{f}_{30} + \bar{f}_{40}. \end{aligned}$$

Here  $\bar{f}_s$  is defined by the  $s$ -th configuration in Table 1 but with a binding strength  $\bar{K}_s$ , given by

$$\bar{f}_s = \frac{\bar{K}_s (K_r x^2)^{i(s)} (K_c y^2)^{j(s)} [RNAP]^{k(s)}}{\sum_{m=1}^{40} \bar{K}_m (K_r x^2)^{i(m)} (K_c y^2)^{j(m)} [RNAP]^{k(m)}}.$$

Except for the configurations indicated in Eq. (5) and (6),  $\bar{K}_s = K_s$  for all other configurations.

## 4. Results

### 4.1. Bistability

It has been indicated that bistability and switching depend not only on the model structure (Cherry and Adler, 2000; Gardner et al., 2000) but also on model parameters. For mathematical models of a mutant system and a wild-type system of  $\lambda$  phage, these systems can traverse between a multistability region and a monostability region with an adjustable parameter (Hasty et al., 2000).

For the network model (7) with threshold values, Fig. 1(A) shows that there are two steady states in the

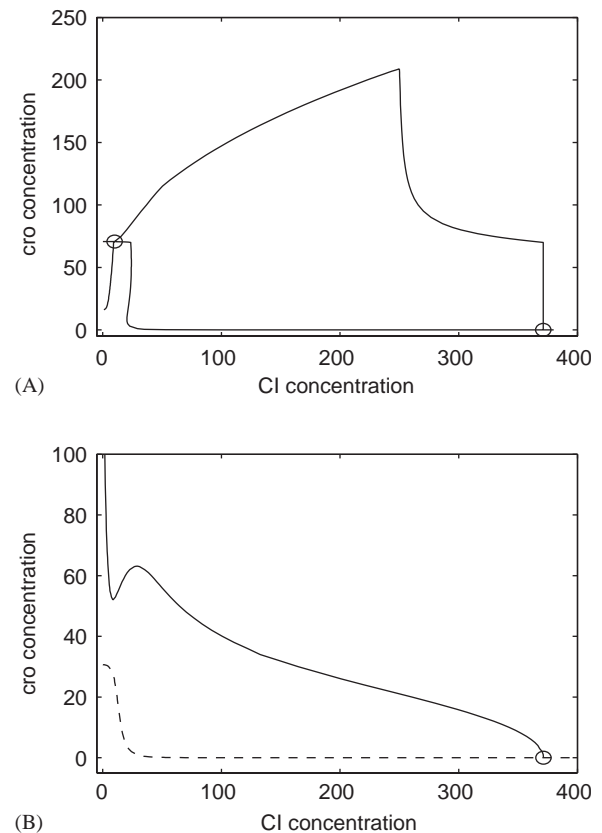


Fig. 1. Null-clines of the deterministic network models. (A) Two steady states exist for the network model (7) with threshold values. (B) A single steady state exists for the network model (2) without any threshold value.

system. In addition, the bistability properties are not sensitive to the choice of threshold values, synthesis rates and degradation rates, which is confirmed by bifurcation analysis and numerical simulations with other nearby parameters. Note that concentrations in the steady states are related to threshold values and other parameters. For example, *cro* concentration in the lysogenic pathway is proportional to the threshold value  $y^*$  and is in inverse proportion to the degradation rate  $k_{dy}$ .

However, Fig. 1(B) indicates that just one single steady state exists with the given data for the network model (2) without any threshold value. The steady state with low CI concentration does not exist and this model could not realize the lysis pathway. Bistability properties of this model depend tightly on model parameters and exist with other control parameters. With the same other control parameters, numerical simulations suggest that bistability exists when  $S_y \geq 51$  for a fixed synthesis rate  $S_x = 6.0$ , or when  $S_x \leq 1.4$  for a fixed synthesis rate  $S_y = 4.7$ . However, these parameters are not consistent with experimental results.

#### 4.2. Genetic switching

When an inducer such as ultraviolet (UV) light is applied to a lysogen, DNA is damaged. This damage leads to a remarkable change in behaviour of the RecA protein which cleaves and inactivates repressors. When there are too few CI dimers binding to the operator sites, polymerase binds to  $P_R$  to begin transcription of *cro*. The induction is realized (Ptashne, 1992).

Similar to the discussion in Hasty et al. (2001a), genetic switching is realized by a large degradation rate of repressor in induction. Fig. 2(A) gives a simulation of successful switching derived from model (7). Using  $k_{dx} = 1.2$  at 60–100 min, repressor concentration decreases considerably and reaches the second steady state. At the same time, *cro* concentration begins to increase and then reaches the steady state of the lysis pathway.

The degradation rate of the repressor should be large enough in order to realize switching. If it is not large enough in model (7), for example  $k_{dx} = 0.8$  at 60–100 min (see Fig. 2(B)), repressor concentration will decrease to  $x = 75$  which is above the threshold value  $x_1^*$ . In this case positive feedback is active and the repressor is still in the fast growth stage. When  $k_{dx}$  returns to the normal value 0.017, positive feedback will stimulate the repressor to bounce back to the steady state with high concentration.

As for the network model (2) without any threshold value, simulation in Fig. 2(C) is different. When a large degradation rate is applied in the lysogenic state ( $k_{dx} = 2.2$  at 60–100 min), the repressor concentration decreases considerably and the *cro* protein level increases at the same time. However, when  $k_{dx}$  returns

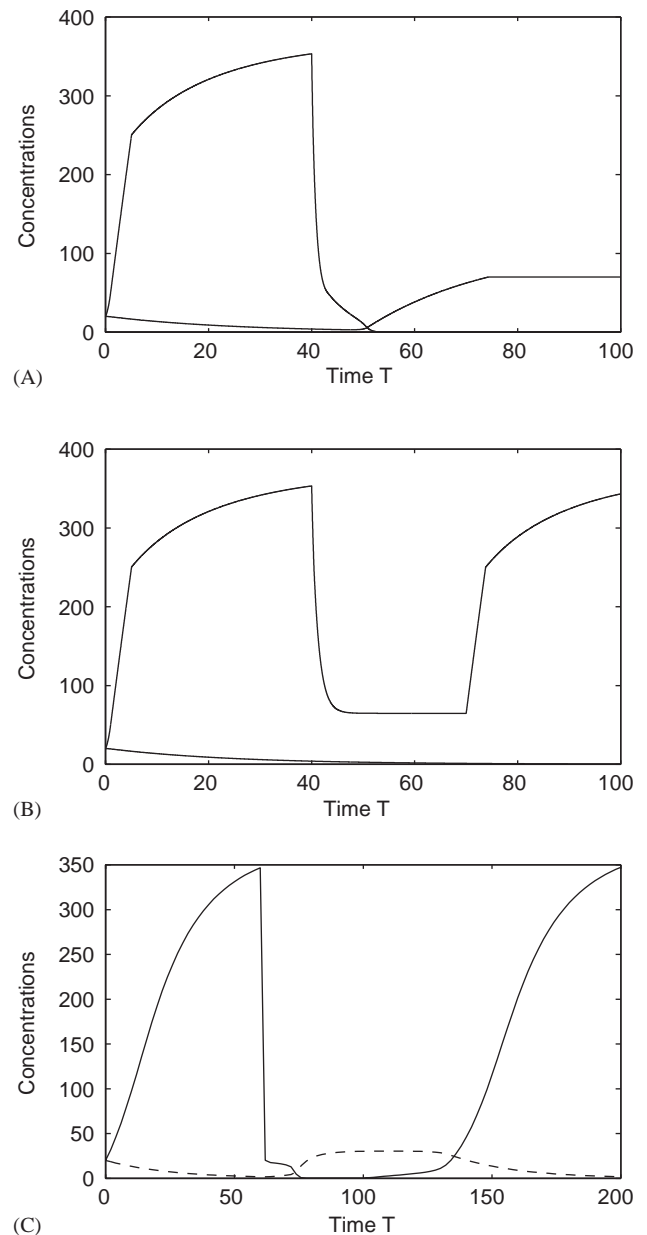


Fig. 2. Simulations of the deterministic network models. (A) A simulation of successful switching by model (7) with degradation rate  $k_{dx} = 1.2$  at 60–100 min. (B) a simulation of unsuccessful switching by model (2) with  $k_{dx} = 0.8$  at 60–100 min. This is due to the degradation rate which is not large enough for induction. (C) A simulation of unsuccessful switching derived from model (2) with  $k_{dx} = 2.2$  at 60–100 min. Bistability does not exist in this model. (CI concentration: solid; *cro* concentration: dashed).

to the normal value 0.017, positive feedback will always stimulate the repressor to bounce back to the steady state with high concentration. This simulation result is consistent with the bistability analysis in Fig. 1(B).

#### 4.3. Stochastic switching

Stochastic models for describing switching mechanisms of  $\lambda$  phage have been studied by introducing

multiplicative noise to the synthesis rate or additive noise (Hasty et al., 2000, 2001a). Although it is recognized that transcription is the most important source of intrinsic noise, we will not study the noise in transcription here due to the space limit and the complexity of the stochastic system. Here we use a stochastic model to realize switching in induction under the influence of intrinsic noise. As the cleavage of repressor is dominant in the process of induction, stochasticity in degradation is more important than other noises in the system. In this case a stochastic degradation rate of repressor is appropriate to realize intrinsic noise in the system.

As with the  $\tau$ -leap method, the number of repressors degraded in the time period  $[t, t + \tau)$  is a Poisson random variable  $P(k_{dx}x\tau)$ , where  $k_{dx}$  is the degradation rate and  $x$  is the present number of the repressor. This assumption also is consistent with that in Thattai and van Oudenaarden (2001). In order to be consistent with the continuous synthesis process, this Poisson random variable is approximated by a Gaussian random variable, namely

$$P(k_{dx}x\tau) \approx N(k_{dx}x\tau, k_{dx}x\tau) \\ = k_{dx}x\tau + \sqrt{k_{dx}x\tau}N(0, 1), \quad (8)$$

where  $N(\mu, \sigma^2)$  is a Gaussian random variable with mean  $\mu$  and variance  $\sigma^2$ . This approximation is valid if the mean of the Poisson random variable is large. This consideration will form the following stochastic equation for describing the stochastic system in induction, given by

$$dx = \bar{S}_x(\bar{P}_x(x, y) - k_{dx}x)dt - \sqrt{k_{dx}x}dW(t), \\ dy = S_y(\bar{P}_y(x, y) - k_{dy}y)dt, \quad (9)$$

where  $W(t)$  is the Wiener process whose increment

$$\Delta W(t) = W(t + \Delta t) - W(t) \sim N(0, \Delta t)$$

is Gaussian.

In order to ensure that the mean of model (9) is the deterministic network model (7), stochastic differential equations are assumed to be of Itô type. In this case, for example, we have that (Van Kampen, 1992)

$$E[\sqrt{k_{dx}x}dW(t)] = 0.$$

Due to small stochastic components, the Euler–Maruyama method (Tian and Burrage, 2001) with stepsize  $\tau = 0.01$  is used for simulating this stochastic model. However, if stochastic components are not small, implicit numerical methods such as the implicit Taylor methods (Tian and Burrage, 2001) should be used in order to guarantee the stability of numerical simulations.

Unlike the simulations derived from the deterministic model (7) (Figs. 2(A) and (B)) where the occurrence of switching is determined by different degradation rates,

the occurrence of switching for the stochastic model is determined by the intrinsic noise in the system (Figs. 3(A) and (B)). With the same control parameters including the repressor degradation rate, the  $\lambda$  phage system may switch from the lysogenic state to the lysis state (Fig. 3(A)) or stay in the lysogenic state (Fig. 3(B)). The key criterion is the decrease of repressor

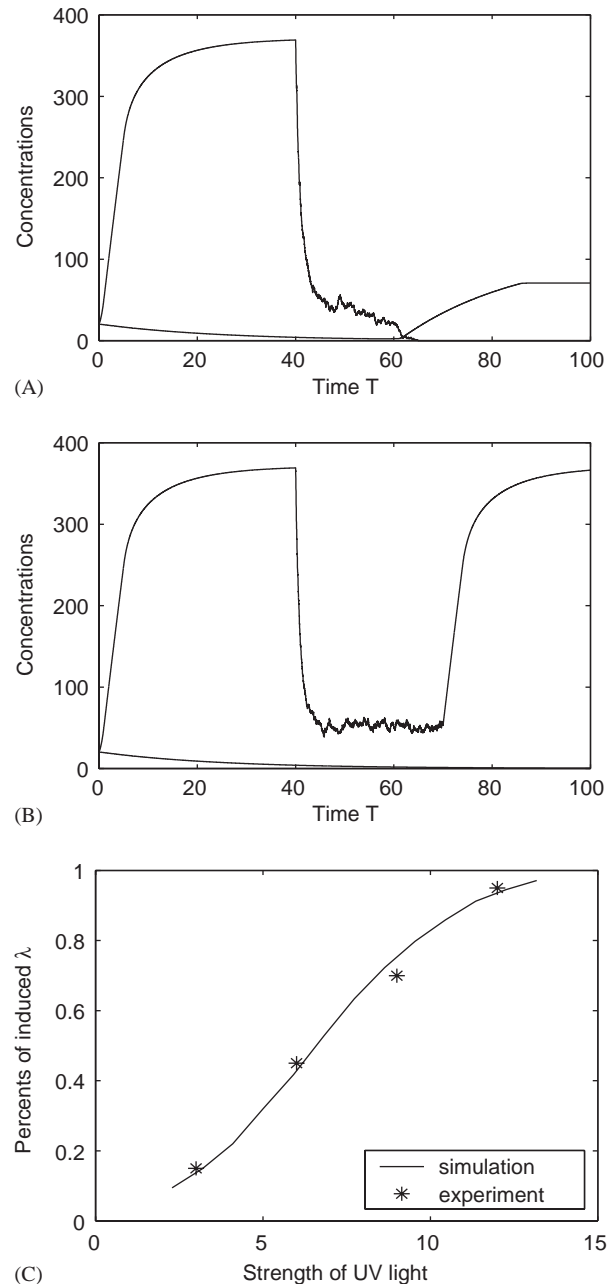


Fig. 3. Simulations and statistical properties of the stochastic model (9). (A) A simulation of successful switching with  $k_{dx} = 1.0$  at 40–70 min. (B) A simulation of unsuccessful switching with the same condition in (A). The occurrence of switching is determined by intrinsic noise in the system. (C) Proportions of the induced  $\lambda$  phage by experiment (four points in \*) and those predicted by simulations with  $k_{dx}$  ranging from 0.99 to 1.11 based on 1000 simulations (solid line).

concentration to about 20% of its original value in the induction period.

The stochastic model (9) can also be used to predict the proportions of the induced  $\lambda$  phage with different strengths of the inducer. Numerical simulations can predict the relationship between the degradation rate and proportions of the induced  $\lambda$  phage. On the other hand, experimental results indicate the relationship between the proportions of the induced  $\lambda$  phage and the strength of the inducer (UV light). We will derive the relationship between the degradation rate and the strength of inducer based on simulation results and experimental data. This data consist of four sets of strengths of UV light and proportions of the induced  $\lambda$  phage which is estimated from the curve labelled  $\lambda_{wt}$  in Fig. 2(C) (Dodd et al., 2001).

Based on 1000 simulations for each degradation rate  $k_{dx}$  ranging from 0.99 to 1.11, we first obtain proportions of the induced  $\lambda$  phage. Numerical results suggest that it is appropriate to use a linear function to express the relationship between the degradation rate of repressor ( $k_{dx}$ ) and strength of UV light ( $U$ ). Based on simulation results and experimental data, the regression line is estimated by the least-square method, with the form

$$k_{dx} = 0.011U + 0.965. \quad (10)$$

Fig. 3(C) indicates that simulation results fit the experimental data quite well.

#### 4.4. Initial conditions

It is known that a single protein CII affects the mechanism for determining developmental pathways (Ptashne et al., 1980; Ptashne, 1992). In those cells in which CII is highly active, lysogeny is established. Otherwise lytic growth ensues if CII is rapidly degraded.

Although the process for establishing developmental pathways is not included in the network model discussed in this paper, the initial condition can be regarded as the outcome of another subsystem for determining the developmental pathway an infecting  $\lambda$  phage follows. The activity of protein CII can be reflected by protein levels of repressor and *cro* as initial conditions. Relatively higher CI protein levels should lead the system to the lysogenic pathway, otherwise the lysis pathway is determined by relatively high *cro* protein levels. Network model (7) can simulate this phenomenon. For example, the initial condition  $x(0) = 5$  and  $y(0) = 10$  can lead to a lysogenic pathway while a lysis pathway can be derived from the initial condition  $x(0) = 5$  and  $y(0) = 20$ . Thus model (7) is capable of incorporating a subsystem for establishing the pathway of an infecting  $\lambda$  phage.

However, model (2) without any threshold values cannot describe this phenomenon. All the initial

conditions will lead to the lysogenic pathway by strong positive feedback that is always effective. This may be regarded as more evidence for the importance of threshold values to realize conditions associated with regulatory mechanisms.

## 5. Conclusions

For biological models with low protein concentrations, an important issue is the assumption of the continuity of concentrations. The key issue is the representation of reactions which occur in low frequencies at a given system state. In this paper we use functions instead of constants to represent binding strengths and synthesis rates in biochemical reactions with low molecule concentrations. The threshold values are used for indicating the effectivity of positive and negative feedback regulatory mechanisms. Using these mathematical representations we construct a quantitative model for describing the evolutionary pathways of  $\lambda$  phage. Bistability and switching are realized by this model with the given experimental data. This model also gives descriptions of different developmental pathways determined by different initial conditions and the decisive mechanism for different pathways in induction.

It should be note that the threshold value in the synthesis rate plays the key role for realizing bistability. Genetic switching cannot be realized if the mechanism of thresholding in positive feedback is not used. On the other hand threshold values in the negative feedback mechanisms are very important for allowing the burst synthesis of proteins. Simulations will approach the steady state much more slowly if it is assumed that negative feedback is always effective.

Stochastic differential equations can be used to describe uncertain phenomena with statistical properties. For the induction from the lysogenic state to the lysis state, a stochastic degradation rate of repressor is used for representing genetic noise within the cells. Numerical simulations can predict the proportionally induced  $\lambda$  phage through a large number of simulations. It has been proposed recently that genetic noise can be used by an organism in deciding between alternative 'states' (Hasty and Collins, 2002). The discussion in this paper is a realization of the effect of genetic noise in deciding developmental pathways of  $\lambda$  phage in induction. It would be very interesting to study the impact of both internal and external noises on genetic regulatory networks at the same time. Another possible stochastic component is through the stochastic initial condition which can be regarded as the output of a stochastic process for determining pathways of the infecting  $\lambda$  phage. It would be interesting to include a stochastic subsystem incorporating this decisive mechanism of



protein CII although a more detailed stochastic kinetic approach has been realized (Arkin et al., 1998).

The simulated percentages of induced  $\lambda$  phage, predicted by model (9) with a stochastic repressor degradation rate, are consistent with experimental data under the assumption of the linear relationship between the strengths of UV light and degradation rates. For the system in the normal condition, namely with zero UV light strength, the stochastic model predicts that 2.3%  $\lambda$  phage will be induced to the lysis pathway with the degradation rate  $k_{dx} = 0.965$  given by Eq. (10). This percentage is consistent with the experimental data (Dodd et al., 2001). However, the degradation rate in this case is not consistent with the experimentally estimated data  $k_{dx} = 0.0173$ . This indicates that the stochastic model based only on degradation rates is not appropriate for describing the system in the normal condition. However, the discussion in this paper is valid for the process of induction when cleavage is the dominant process of the system. For a biological system without any irradiation, genetic noise in transcription is also very important for determining the developmental pathway of  $\lambda$  phage. Thus the discussion of genetic noise in this paper is not complete for the system in the normal condition and more work is needed for studying genetic noise in both transcription and degradation. In addition more work is also needed for studying mutant systems of  $\lambda$  phage by excluding certain configurations from the complete list in Table 1. However, due to the limit of space and complexities of these problems, these issues are prospective topics for future work.

## References

- Ackers, G.K., Johnson, A.D., Shea, M.A., 1982. Quantitative model for gene regulation by  $\lambda$  phage repressor. *Proc. Natl. Acad. Sci. USA* 79, 1129–1133.
- Alon, U., Surette, M.G., Barkai, N., Leibler, S., 1999. Robustness in bacterial chemotaxis. *Nature (London)* 397, 168–171.
- Arkin, A., Ross, J., McAdams, H.H., 1998. Stochastic kinetic analysis of developmental pathway bifurcation in phage lambda-infected *Escherichia coli* cells. *Genetics* 149, 1633–1648.
- Barkai, N., Leibler, S., 1997. Robustness in simple biochemical networks. *Nature (London)* 387, 913–917.
- Becskei, A., Serrano, L., 2000. Engineering stability in gene networks by autoregulation. *Nature (London)* 405, 590–593.
- Cherry, J.L., Adler, F.R., 2000. How to make a biological switch. *J. Theor. Biol.* 203, 117–133.
- Darling, P.J., Holt, J.M., Ackers, G.K., 2000. Coupled energetics of  $\lambda$  *cro* repressor self-assembly and site-specific DNA operator binding II: cooperative interactions of *cro* dimers. *J. Mol. Biol.* 302, 625–638.
- Dodd, I.B., Perkins, A.J., Tsemitsidis, D., Egan, J.B., 2001. Octamerization of  $\lambda$  cI repressor is needed for effective repression of  $P_{RM}$  and efficient switching from lysogeny. *Genes Dev.* 15, 3013–3022.
- Gardner, T.S., Collins, J.J., 2000. Neutralizing noise in gene networks. *Nature (London)* 405, 520–521.
- Gardner, T.S., Cantor, C.R., Collins, J.J., 2000. Construction of a genetic toggle switch in *Escherichia coli*. *Nature (London)* 403, 339–342.
- Gillespie, D.T., 1977. Exact stochastic simulation of coupled chemical reactions. *J. Phys. Chem.* 81, 2340–2361.
- Gillespie, D.T., 2001. Approximate accelerated stochastic simulation of chemically reacting systems. *J. Chem. Phys.* 115, 1716–1733.
- Gonze, D., Halloy, J., Goldbeter, A., 2002. Robustness of circadian rhythms with respect to molecular noise. *Proc. Natl. Acad. Sci. USA* 99, 673–678.
- Hasty, J., Collins, J.J., 2002. Translating the noise. *Nature Genet.* 31, 13–14.
- Hasty, J., Pradines, J., Dolnik, M., Collins, J.J., 2000. Noise-based switches and amplifiers for gene expression. *Proc. Natl. Acad. Sci. USA* 97, 2075–2080.
- Hasty, J., Issacs, F., Dolnik, M., McMillen, D., Collins, J.J., 2001a. Design gene network: towards fundamental cellular control. *Chaos* 11, 207–220.
- Hasty, J., McMillen, D., Isaacs, F., Collins, J.J., 2001b. Computational studies of gene regulatory networks: in numero molecular biology. *Nat. Rev. Genet.* 2, 268–279.
- Johnson, A.D., Poteete, A.R., Lauer, G., Sauer, R.T., Ackers, G.K., Ptashne, M., 1981.  $\lambda$  repressor and *cro*-components of an efficient molecular switch. *Nature (London)* 294, 217–223.
- Van Kampen, N.G., 1992. *Stochastic Processes in Physics and Chemistry*. North-Holland, Amsterdam.
- Maurer, R., Meyer, B.J., Ptashne, M., 1980. Gene regulation at the right operator  $\{O_P\}$  of bacteriophage  $\lambda$ , I.  $O_{R3}$  and autogenous negative control by repressor. *J. Mol. Biol.* 139, 147–161.
- McAdams, H.H., Arkin, A., 1997. Stochastic mechanism in gene expression. *Proc. Natl. Acad. Sci. USA* 94, 814–819.
- Meyer, B.J., Maurer, R., Ptashne, M., 1980. Gene regulation at the right operator  $\{O_P\}$  of bacteriophage  $\lambda$ , II  $O_{R1}$ ,  $O_{R2}$  and  $O_{R3}$ : their roles in mediating the effects of repressor and *cro*. *J. Mol. Biol.* 139, 163–194.
- Ptashne, M., 1992. *A Genetic Switch: Phage  $\lambda$  and Higher Organisms*, 2nd Edition. Cell Press, Cambridge, MA.
- Ptashne, R., Jeffrey, A., Johnson, A.D., Maurer, R., Meyer, B.J., Pabo, C.O., Roberts, T.M., Sauer, R.T., 1980. How the  $\lambda$  repressor and *cro* work. *Cell* 19, 1–11.
- Reinitz, J., Vaisnys, J.R., 1990. Theoretical and experimental analysis of the phage lambda genetic switch missing levels of co-operativity. *J. Theor. Biol.* 145, 295–318.
- Shea, M.A., Ackers, G.K., 1985. The  $O_R$  control system of bacteriophage Lambda: a physical-chemical model for gene regulation. *J. Mol. Biol.* 181, 211–230.
- Smolen, P., Baxter, D.A., Byrne, J.H., 2000. Mathematical modelling of gene networks. *Neuron* 26, 567–580.
- Thattai, M., van Oudenaarden, A., 2001. Intrinsic noise in gene regulatory networks. *Proc. Natl. Acad. Sci. USA* 98, 8614–8619.
- Tian, T., Burrage, K., 2001. Implicit Taylor methods for stiff stochastic differential equations. *Appl. Numer. Math.* 38, 167–185.